HHS Public Access

Author manuscript

J Bone Miner Res. Author manuscript; available in PMC 2020 March 01.

Published in final edited form as:

J Bone Miner Res. 2019 March ; 34(3): 533–546. doi:10.1002/jbmr.3615.

Inactivation of Nell-1 in chondrocytes significantly impedes appendicular skeletogenesis

Huichuan Qi, DDS, MS[1,2], **Jong Kil Kim, BS**[2], **Pin Ha, DDS, MD**[2], **Xiaoyan Chen, DDS, PhD**[2,3], **Eric Chen, DDS**[2], **Yao Chen, DDS, MS**[2], **Jiayi Li, MS**[2], **Hsin Chuan Pan, DDS**[2], **Mengliu Yu, DDS, PhD**[2,4], **Yasamin Mohazeb, BS**[2], **Sophia Azer, BS**[2], **Lloyd Baik, BS**[2], **Jin Hee Kwak, DDS, MS**[2], **Kang Ting, DMD, DMedSc**[2,*], **Xinli Zhang, MD, PhD**[2,*], **Min Hu, DDS, PhD**[1,*], **Chia Soo, MD**[5,*]

[1]Department of Orthodontics, School and Hospital of Stomatology, Jilin University, Changchun, Jilin, P. R. China

[2]Division of Growth and Development, Section of Orthodontics, School of Dentistry, University of California, Los Angeles, California, USA

[3]Department of Orthodontics, Affiliated Hospital of Stomatology, Medical College, Zhejiang University, Hangzhou, Zhejiang, P. R. China

[4]Center of Stomatology, China-Japan Friendship Hospital, 2nd Yinghuayuan East Street, Chaoyang District, Beijing, P. R. China

[5]Division of Plastic and Reconstructive Surgery and Department of Orthopaedic Surgery and the Orthopaedic Hospital Research Center, University of California, Los Angeles, Los Angeles, California, USA

Abstract

NELL-1, an osteoinductive protein, has been shown to regulate skeletal ossification. Interestingly, an interstitial 11p14.1-p15.3 deletion involving the Nell-1 gene was recently reported in a patient with short stature and delayed fontanelle closure. Here we sought to define the role of Nell-1 in endochondral ossification by investigating Nell-1-specific inactivation in Col2α1 expressing cell lineages. Nell-$1^{flox/flox}$; Col2α1-Cre^{+} (Nell-$1^{Col2\alpha1}$KO) mice were generated for comprehensive analysis. Nell-$1^{Col2\alpha1}$KO mice were born alive but displayed subtle femoral length shortening. At 1 and 3 months postpartum, Nell-1 inactivation resulted in dwarfism and premature osteoporotic phenotypes. Specifically, Nell-$1^{Col2\alpha1}$KO femurs and tibias exhibited significantly reduced length, BMD, BV/TV, trabecular number/thickness, cortical volume/thickness/density, and increased trabecular separation. The decreased bone formation rate revealed by dynamic histomorphometry was associated with altered numbers and/or function of osteoblasts and osteoclasts. Furthermore,

[*]**Corresponding Address:** Dr. Xinli Zhang. Research Director and Professor, Section of Orthodontics, Division of Growth and Development. School of Dentistry, University of California, Los Angeles, 10833 Le Conte Ave, Los Angeles, CA90095, Office Phone#: 310-794-5479, xzhang@dentistry.ucla.edu.

Author contributions: Xinli Zhang, Kang Ting, Chia Soo, and Min Hu conceived and designed the study, interpreted data, and approved the manuscript; Huichuan Qi, Jong Kil Kim, Pin Ha, Xiaoyan Chen, Yao Chen, Jiayi Li, and Xinli Zhang executed the study, collected and analyzed the data, and wrote the manuscript; Eric Chen, Hsin Chuan Pan, Mengliu Yu collected and analyzed the data, and edited the manuscript; Yasamin Mohazeb, Sophia Azer, Lloyd Baik, and Jin Hee Kwak collected the data.

Supplementary data: This submission includes 3 supplementary tables, 7 supplementary figures and their legends.

longitudinal observations by *in vivo* micro-CT showed delayed and reduced mineralization at secondary ossification centers in mutants. Histologically, reduced staining intensities of Safranin O, Col-2, Col-10, and fewer BrdU-positive chondrocytes were observed in thinner Nell-1$^{Col2\alpha1}$KO epiphyseal plates along with altered distribution and weaker expression level of Ihh, Patched-1, PTHrP, and PTHrP receptor. Primary Nell-1$^{Col2\alpha1}$KO chondrocytes also exhibited decreased proliferation and differentiation, and its downregulated expression of the Ihh-PTHrP signaling molecules can be partially rescued by exogenous Nell-1 protein. Moreover, intra-nuclear Gli-1 protein and gene expression of the Gli-1 downstream target genes, Hip-1 and N-Myc, were also significantly decreased with Nell-1 inactivation. Notably, the rescue effects were diminished/reduced with application of Ihh signaling inhibitors, cyclopamine or GANT61. Taken together, these findings suggest that Nell-1 is a pivotal modulator of epiphyseal homeostasis and endochondral ossification. The cumulative chondrocyte-specific Nell-1 inactivation significantly impedes appendicular skeletogenesis resulting in dwarfism and premature osteoporosis through inhibiting Ihh signaling and predominantly altering the Ihh-PTHrP feedback loop.

Keywords

Nell-1; conditional knockout mouse model; endochondral ossification; epiphyseal homeostasis; Ihh-PTHrP signaling loop

Introduction

Nell-1 was originally identified as a craniosynostosis-associated molecule from resected human coronal sutures with strong evidence from Nell-1-overexpression transgenic mouse models [1,2]. Recently, a Nell-1 gene single-nucleotide polymorphism was identified as a susceptible factor for human osteoporosis [3]. The osteoporotic phenotype has concomitantly been observed in senile haploinsufficient Nell-1 mutant mice induced by *N*-ethyl-*N*-nitrosourea (ENU) [4]. More recently, the first clinical case associated with an interstitial deletion of 11p14.1-p15.3 involving Nell-1 was reported in a 3-year-old Japanese girl with short stature and delayed fontanelle closure [5]. At 3 years and 7 months of age, her height was 83.8 cm, far below average (−3.5 SD). Besides these studies implicating the Nell-1 gene with various phenotypes, our previous studies have also shown that Nell-1 holds promising therapeutic potential in the regeneration of bone and cartilage as revealed in numerous preclinical animal models with Nell-1 application ranging from rodents to non-human primates [6–11]. Therefore, Nell-1 is among the functional key factors in modulating skeletogenesis and warrants further in-depth mechanistic research. However, a homozygous ENU-induced point mutation in the mouse Nell-1 gene results in neonatal death [12]. Consequently, it is important to generate a genetically modified Nell-1 mutant model that can overcome neonatal lethality and allow for defined investigation of Nell-1 inactivation in osteochondral tissues at the postnatal stage. The successful creation of floxed Nell-1 mice using the Cre-LoxP system makes such defined investigation possible to advance our current understanding on the pro-osteogenic role of Nell-1.

Historically, previous research has focused on revealing the role of Nell-1 in the development of craniofacial skeletons [1,2,8,12–15]. In contrast to intramembranous bone

formation in craniofacial osteogenesis, endochondral ossification is an essential process for the development and elongation of the appendicular bones. Undisputedly, the epiphyseal plate is frequently subject to pathologic anomalies of skeletal growth and development. This is primarily due to the fact that the behavior of epiphyseal plate chondrocytes plays a vital role in regulating all stages of endochondral ossification through a complex network of hormones, growth factors, and components of extracellular matrix [16]. It is crucial to maintain homeostasis of the proliferation, differentiation, and maturation of chondrocytes within the epiphyseal plate for long bone growth [17,18]. Among the numerous growth factors and signaling molecules identified thus far in regulating epiphyseal plate homeostasis, the Hedgehog signaling pathway acts as a master regulator [19–22]. Among the three Hedgehog proteins in mammals, Indian hedgehog (Ihh) is known to induce major biological impacts on both chondrocyte and osteoblast differentiation during endochondral ossification [23]. It can also stimulate chondrocyte proliferation directly and plays a critical role in regulating the onset of chondrocyte hypertrophy by forming a negative feedback loop with Parathyroid hormone-related protein (PTHrP) [24]. It is important to note that Nell-1 is capable of elevating Ihh gene expression in Runx2 null chondrocytes to compensate for the developmental deficiency of chondrogenic differentiation [25,26]. Consequently, it is highly expected that specific inactivation of Nell-1 in chondrocytes will significantly alter the homeostasis of the epiphyseal plate, thereby affecting appendicular bone growth. Although this topic has yet to be explored, some phenotypic observations of the osteoporotic bone condition have been found in senile ENU-induced haploinsufficient Nell-1deficient mice (END mice) [4].

In this study, we aim to reveal the role of Nell-1 in the growth and maintenance of the appendicular bones using a conditional Nell-1 knockout with Col2α1-Cre in chondrocytes expressing Collagen type 2 (Col-2). First, the skeletal phenotypic changes of Nell-1 mutants were systemically evaluated in multiple stages upon confirmation of specific inactivation of Nell-1 in Col-2 expressing chondrocytes. The epiphyseal plate was then studied extensively to reveal histological changes, chondrocyte proliferation and differentiation, and Ihh-PTHrP signaling alteration in Nell-1 mutants compared to wild type control mice. Furthermore, to better reveal Nell-1's functionality in endochondral ossification, mineralization at secondary ossification centers and changes of femoral and tibial lengths were observed longitudinally (from postnatal day 7 to day 28 as similarly reported [27]) by *in vivo* micro-CT. In addition, dynamic histomorphometry of the metaphyseal trabecular bones of the femur and tibia was performed at 1 and 3 months postpartum. Finally, the molecular mechanisms underlying the significant alterations of the appendicular bones in Nell-1 knockout mutants were further delineated using an *in vitro* system of primary chondrocytes with gain and loss of Nell-1 and the relevant Ihh signaling inhibitors. Here we show for the first time that Nell-1 inactivation in Col-2 expressing chondrocytes resulted in short stature/dwarfism and premature osteoporosis, implying that Nell-1 is essential in modulating epiphyseal homeostasis and appendicular skeletogenesis.

Materials and Methods

Generation of chondrocyte-specific Nell-1 knockout

Nell-1 floxed mice (Nell-$1^{flox/flox}$) were generated by flanking Exon 1 containing ATG site with loxP and then excising the FRT-flanked Neo cassette with FLPo-10 delete mice (Stock# 011065, Jackson Laboratory) in C57BL/6J background. The frozen embryos of Nell-$1^{flox/flox}$ mice (EM: 04309; Strain: B6.129Sv/Pas-Nell1tm) were purchased from European Mouse Mutant Archive (EMMA), and the rederivation was performed by the ART Lab of the University of California, Los Angeles (UCLA). To delete Nell-1 specifically in chondrocytes, Nell-$1^{flox/flox}$; Col2α1-Cre^{+} (Nell-$1^{Col2α1}$KO) mice were generated by crossing Nell-$1^{flox/flox}$ mice and Col2α1-Cre transgenic mice (Stock# 003554, Jackson Laboratory). Cre negative littermates were used as wild type mice (WT), while Col2α1-Cre transgenic mice were used as a negative control (Col2-Cre+). In order to monitor Col2α1-Cre expression at target locations, Nell-$1^{Col2α1}$KO mice were mated with ROSA26 mice (Stock# 003474, Jackson Laboratory) to yield Nell-$1^{flox/flox}$; Col2α1-Cre^{+}; $R26R^{+}$ (Nell-$1^{Col2α1\text{-}R26R}$KO) mice and Nell-$1^{flox/flox}$; Col2α1-Cre^{-}; $R26R^{+}$ littermates as WT. Mouse genotypes were identified by DNA extraction and amplification. All animals were cared for according to institutionally approved protocols provided by the Chancellor's Animal Research Committee at UCLA (protocol number: 2012-041).

Micro-Computed Tomography (micro-CT) analyses

***Ex vivo* scanning:** Skeletons of newborn pups (P0), 1-month and 3-month femur and tibia were imaged *ex vivo* in a high resolution micro-CT scanner (Skyscan 1172, Bruker-microCT, Konitch, Belgium) as previously described [(4)].

***In vivo* scanning:** Both sides of the femur and tibia of the same mice were repeatedly scanned *in vivo* using a micro-CT scanner (Skyscan 1176, Bruker-microCT, Konitch, Belgium) at postnatal day 7, 14, 21, and 28 to longitudinally observe secondary ossification center (SOC) formation and changes in the length of limbs. The images were scanned with the setting of 18μm pixel size, 50kV Voltage, 500μA current, 0.5mm Al filter, 250 ms exposure time, 0.600 rotation step, and no frame averaging.

Data analysis: The scanned images were reconstructed by NRecon (Version 1.7.1.0, Bruker-microCT, Kontich, Belgium) with the setting of 50% Bean Hardening Correction, 3 Smoothing (Gaussian), and 20 Ring Artifact Correction. The reconstructed images were aligned in parallel to the vertical axis via Data Viewer (Version 1.5.2.4 64 bit, Bruker-microCT, Kontich, Belgium). For detailed analysis, CTAn (Version 1.16.4.1 64 bit, Bruker-microCT, Kontich, Belgium) was used in global threshold of 80. For trabecular bone analysis, a 2mm region of interest (ROI) was selected above the epiphyseal plate of the distal femur and proximal tibia. For cortical bone analysis, 1mm of the midshaft of the femur and tibia were selected as the ROI. Parameters including bone mineral density (BMD), bone volume/tissue volume (BV/TV), trabecular number (Tb-N), trabecular thickness (Tb-Th), trabecular separation (Tb-Sp), cortical bone volume (CB-V), thickness (CB-Th) and cortical bone mineral density (CBMD) were analyzed within the defined ROI. 3D models (STL

format) of the femur and tibia were generated, and were imported to MeshLab (v1.3.2_64bit, Visual Computing Lab - ISTI - CNR) for 3D length analysis.

Dynamic histomorphometric analyses

Mice at 1 month and 3 months were injected intraperitoneally with Calcein (20 mg/kg) and Alizarin Red Complexon (50 mg/kg) at 9 and 2 days before sacrifice, respectively. The femur and tibia were dissected and fixed in 70% ethanol. Undecalcified frozen sections were cut following Kawamoto's procedure [28] and analyzed using the OsteoMeasure morphometry system (Osteometrics). The mineral apposition rate (MAR) and bone formation rate per unit of bone surface (BFR/BS) were calculated as previously described [4]. All image acquisitions and analyses were performed in a blinded manner.

Skeletal analyses

Double transgenic newborn offspring, WT and Nell-1$^{Col2\alpha1\text{-}R26R}$KO pups, were dissected for whole-mount X-gal staining. After euthanization, newborn WT and Nell-1$^{Col2\alpha1}$KO pups were dissected by carefully removing the skin and fixed in 95% ethanol for 12-48 hours, followed by staining with Alcian Blue solution and Alizarin Red solution to visualize the skeletons. The femur and tibia were harvested at different stages for morphological evaluation.

Histological analyses and immunohistochemistry

Paraffin-sections were used for H&E staining, Safranin O staining and immunohistochemistry (IHC) following the standard protocols[29]. To further confirm Nell-1 deletion at the tissue level, a specific Nell-1 antibody was applied on neonatal tibia by IHC along with X-gal staining. TRAP staining and IHC for Osteocalcin (OCN) were used for differentiate osteoclasts (OC) and osteoblasts (OB), respectively. To assay *in vivo* cell proliferation, BrdU (00-0103, Invitrogen) was intraperitoneally injected at 1ml per 100g body weight 2 hours before sacrifice. BrdU incorporation was detected by IHC. Four random fields in the tibial epiphyseal proliferation zone were taken from each slide and positive cells were quantified using Image-Pro Plus software. Average each slide for statistics. Primary antibodies used for IHC were listed in Suppl Table S1.

Isolation and cultivation of mouse primary sternal chondrocytes

Primary sternal chondrocytes were isolated and used in this study similar to previous comparable studies [30,31]. In addition, similar gene expression profiles between primary sternal chondrocytes and lower extremity chondrocytes (articular chondrocytes) were observed in our initial screening (data not shown). After removing soft tissues by 2 mg/ml protease (P6911, Sigma-Aldrich) and 3 mg/ml collagenase (C6885, Sigma-Aldrich), the rib cages of newborn pups were digested in 0.3 mg/ml collagenase for 3 hours to achieve single-cell suspension for expansion in culture medium (DMEM with 10% FBS, 100 U/ml penicillin, and 100 μg/ml streptomycin). Passage 1 (P1) WT and Nell-1$^{Col2\alpha1}$KO chondrocytes were used for 14-day cultivation in chondrogenic medium (DMEM with 5% FBS, 100 U/ml penicillin, 100 μg/ml streptomycin, 1% ITS, 100 nM Dexamethasone, and 50 μg/ml ascorbic acid) with or without 1000 ng/ml recombinant human NELL-1

(rhNELL-1) for Alcian blue staining and real-time PCR. For quantification, Alcian blue staining was solubilized in 1% SDS, and the absorbance was measured at 605nm. P1 WT and Nell-1$^{Col2\alpha1}$KO chondrocytes were also cultured for 3 days for quantitative real-time PCR, immunocytochemistry (ICC), and Western blot analyses with presence of 1000 ng/ml rhNELL-1, 5μM GANT61 (ab120904, Abcam), 10μM Cyclopamine (ab120392, Abcam) alone or in combination. MTT assay was performed with P1 WT and Nell-1$^{Col2\alpha1}$KO chondrocytes with or without 1000 ng/ml rhNELL-1 at day 0, 2, 4 and 6.

Western blot and Real-time quantitative PCR

Western blot analysis was performed as previously described [4,32]. Briefly, nuclear and cytoplasmic proteins were isolated using an NE-PER Nuclear and Cytoplasmic Extraction Kit (Thermo Scientific). Primary antibodies listed in Suppl Table S2 were used at different concentrations for Western blot analyses. Real-time PCR was performed on the QuantStudio 3 Real-Time PCR system (Applied Biosystems) with SYBR Green Master mix (Applied Biosystems). All primer sequences used were listed in Suppl Table S3. GAPDH was detected as housekeeping standard. Relative gene expression was analyzed by ΔΔCT method.

Statistical analysis

All quantifiable data were presented as mean ± SD. A Shapiro-Wilk test for normality was performed on all data sets. Homogeneity was confirmed by a comparison of variance test. Statistical significance was analyzed using the Student's t-test when two groups were compared or using a one-way analysis of variance test when more than two groups were compared, followed by a *post hoc* Tukey's test to compare the two groups. A value of $p<0.05$ was regarded as statistically significant. Statistical analyses were consulted with the UCLA Statistical Biomathematical Consulting Clinic.

Results

Specific inactivation of Nell-1 in Collagen Type 2 expressing cells inhibits the full potential of mouse limb development

Nell-1 inactivation in Col-2 expressing cells (Nell-1$^{Col2\alpha1}$KO) was obtained by cross mating Nell-1$^{flox/flox}$ mice, which were generated using the standard Cre-LoxP technique, with Col2α1-Cre driver mice [33]. Conditional Nell-1 knockout in Col-2 expressing cells did not result in embryonic and neonatal lethality and did not affect mouse fertility. Breeding of Nell-1$^{Col2\alpha1}$KO mice was according to a Mendelian distribution in general. The targeted location of Nell-1 inactivation was first demonstrated by cartilage-specific whole-mount X-gal staining in Nell-1$^{Col2\alpha1\text{-}R26R}$KO mice (Fig. 1A). Positive X-gal staining was observed in the cartilage end of newborn tibia and also at 1-month and 3-month epiphyseal plates (Suppl Fig. S1). Chondrocyte-specific deletion of Nell-1 was then quantified by quantitative real-time PCR, showing a significant decrease of Nell-1 in primary Nell-1$^{Col2\alpha1}$KO chondrocytes but not in primary calvarial cells (Fig. 1B). Furthermore, Nell-1 deletion at the tissue level was demonstrated by double staining of Nell-1 and X-gal. The distinct location and tissue distribution of positive Nell-1 and X-gal staining in WT and Nell-1$^{Col2\alpha1\text{-}R26R}$KO samples validated that Nell-1 inactivation was profound in chondrocytes *in vivo* (Fig. 1C).

Grossly, the subtle shortness of limbs seen in Nell-1$^{Col2\alpha1}$KO mice was only appreciable by limb length measurements based on skeletal staining and micro-CT scanning (Fig. 1D), while no difference was observed between WT and Col2-Cre+ mice (Suppl Fig. S2). Histologically, there was no detectable morphological differences in the zonal chondrocyte band widths between WT and Nell-1$^{Col2\alpha1}$KO mesial tibias (Fig. 1E). However, BrdU positive cells were observed much less in Nell-1$^{Col2\alpha1}$KO samples (Fig. 1F). The staining intensities of Safranin O and Col-2 were drastically reduced while Col-10 expression was hardly detectable in Nell-1$^{Col2\alpha1}$KO samples (Fig. 1G). Moreover, the hindlimb explants from E16.5 Nell-1$^{Col2\alpha1}$KO mice treated with or without recombinant Nell-1 protein validated the necessity of Nell-1 in limb development and growth through affecting chondrocyte proliferation and maturation (Suppl Fig. S3). Thus, inactivation of Nell-1 in Col-2 expressing cells affects chondrocyte proliferation and full differentiation potential, also leading to insufficient development of the limbs.

Lack of Nell-1 in chondrocytes results in dwarfism and premature osteoporotic phenotypes

The short stature of Nell-1$^{Col2\alpha1}$KO mice was readily recognizable in comparison to WT littermates at 1 and 3 months, respectively (Fig. 2A, B). The body length and tail length were all significantly shorter in Nell-1$^{Col2\alpha1}$KO compared to WT mice (Fig. 2C), while no difference was observed between the WT and Col2-Cre+ control groups (Suppl Fig. S4A). In addition, the average body weight of Nell-1$^{Col2\alpha1}$KO mice was lighter than that of WT controls (Suppl Fig. S4B). Significantly, femur and tibia lengths were much shorter and the bone mineral density was reduced in Nell-1$^{Col2\alpha1}$KO mice as measured by quantitative micro-CT measurements and density distributions (Fig. 2D, E). 3D reconstructions of the femur and tibia revealed that they were shorter and smaller, while the trabecular bones in the metaphyseal areas of the distal femur and proximal tibia exhibited osteoporotic phenotypes in Nell-1$^{Col2\alpha1}$KO mice at both 1 and 3-month stages (Fig. 2F, G). ROIs are shown in Suppl Fig. S4C. Similar data obtained from the WT and Col2-Cre+ control groups are shown in Suppl Fig. S4D–K. Correspondingly, morphometric analyses further confirmed significant reductions in the bone volume (BV/TV), trabecular thickness (Tb-Th) and trabecular number (Tb-N) in Nell-1$^{Col2\alpha1}$KO mice, in addition to increased trabecular separation (Tb-Sp) (Fig. 2F, G). Besides, the cortical bone volume, thickness, and mineral density were also measured (Suppl Fig. S5A, B). At 1 month, these metrics were all significantly decreased in Nell-1$^{Col2\alpha1}$KO mice. While at 3 months, although Nell-1$^{Col2\alpha1}$KO mice still showed a significant reduction in cortical bone volume and thickness, no difference in mineral density was observed in comparison to WT mice, both in males and in females.

Histologically, chondrocyte organization in the epiphyseal plate of 1-month-old Nell-1$^{Col2\alpha1}$KO was apparently different from the column-aligned arrangement seen in WT mice (Fig. 3A). Moreover, the thickness of the epiphyseal plate was significantly thinner in Nell-1$^{Col2\alpha1}$KO compared to WT mice at both 1 and 3 months (Fig. 3B, C). Notably, a narrower proliferative zone of chondrocytes was observed in 1-month-old Nell-1$^{Col2\alpha1}$KO mice. In addition to reduced expression of the chondrogenic markers, Safranin O, Col-2 and Col-10 (Fig. 3A), the number of proliferating cells as identified by BrdU labeling were significantly reduced in 1-month-old Nell-1$^{Col2\alpha1}$KO mice (Fig. 3D). Thus, the lack of Nell-

1 in chondrocytes affects endochondral bone formation resulting in dwarfism and osteoporotic phenotypes.

Nell-1$^{Col2\alpha1}$KO mutants have reduced bone growth rate and delayed mineralization at secondary ossification centers

Because of the metaphyseal osteoporotic phenotype observed in both the femur and tibia in Nell-1$^{Col2\alpha1}$KO mice, standard bone labelling and dynamic histomorphometric analyses were performed with 1-month-old and 3-month-old femur and tibia to calculate definitively the effects on bone growth with Nell-1 inactivation in chondrocytes. Apparently, both MAR and BFR/BS were significantly reduced in Nell-1$^{Col2\alpha1}$KO mice compared with WT littermates at these two postnatal stages (Fig. 4A, B). There was no statistical difference between the WT and Col2-Cre+ control groups in both male and female mice (Suppl Fig. 5C). Moreover, the quantifications of the numbers of OB and OC based on OCN and TRAP staining revealed significantly reduced OB and increased OC in 3-month-old Nell-1$^{Col2\alpha1}$KO mice, but no significant difference in 1-month-old mice (Fig. 4C, D). This may indicate that the functional deficit of osteoblasts and osteoclasts was the major cause for the osteoporotic phenotype observed in 1-month-old Nell-1$^{Col2\alpha1}$KO mice, while in the later stage of 3 months, both a functional deficit and the absolute number of osteoblasts and osteoclasts were responsible for the osteoporotic phenotype. Indeed, the differences of MAR and BFR/BS between Nell-1$^{Col2\alpha1}$KO and WT mice were greater in 3-month-old mice than in 1-month-old mice (Fig. 4A, B).

To further determine if Nell-1 inactivation in chondrocytes is directly involved in endochondral ossification, *in vivo* micro-CT was conducted to observe SOC formation and the changes in length of the femur and tibia at different time points during postnatal development. SOC was first detected only in P7 WT femurs as reported in previous studies [27,30], but not in Nell-1$^{Col2\alpha1}$KO femurs of the same litter nor in WT and Nell-1$^{Col2\alpha1}$KO tibias by 3D reconstructions (Fig. 4E, F). The dynamic changes in bone volume and length of the femur and tibia were clearly captured by live micro-CT imaging and quantitative measurements. Although SOC bone volume and length of the femur and tibia increased with time in both WT and Nell-1$^{Col2\alpha1}$KO mice, Nell-1$^{Col2\alpha1}$KO mice had significantly smaller SOC volume and shorter femur and tibia at each studied time point in comparison to WT littermates. Interestingly, the differential degree of SOC bone volume between KO and WT mice at all indicated time points remain much greater than that of bone length. This may further indicate the strong effect of Nell-1 inactivation on endochondral bone formation in SOC in addition to its effect on growth of the epiphyseal plate at these postnatal stages. Notably, the intensity and distribution of VEGF, Col-10, and Runx2 immunostaining were significantly altered at postnatal day 7 (P7) of the initial stage of SOC formation in Nell-1$^{Col2\alpha1}$KO mice (Fig. 4G, H). These reduced expressions *in vivo* were consistent with the gene expression levels observed in primary WT and Nell-1$^{Col2\alpha1}$KO chondrocytes, while application of exogenous rhNELL-1 significantly rescued this loss (Suppl Fig. S6).

Collectively, these results demonstrated that Nell-1 inactivation in Col-2 expressing chondrocytes leads to significantly delayed formation of secondary ossification centers and a much-reduced growth rate of the appendicular bones.

Nell-1 is essential in maintaining a balanced Ihh-PTHrP loop in the epiphyseal plate

Since Ihh is a key regulator during endochondral ossification and can form a feedback loop with PTHrP, we next studied the expression patterns of Ihh and PTHrP together with their receptors Patched-1 (Ptch) and PTHrP receptor (PTHrP-R) on the tibial epiphyseal plates of newborn (P0) and 1-month-old WT and Nell-1$^{Col2\alpha1}$KO mice. At the newborn stage, Ihh (Fig. 5A), Patched-1 (Fig. 5B), and PTHrP-R (Fig. 5D) were all observed in the prehypertrophic and early hypertrophic chondrocytes, while PTHrP (Fig. 5C) was only observed on the top, expressed by perichondrial cells and resting chondrocytes. The Nell-1$^{Col2\alpha1}$KO epiphyseal plate showed narrower ranges and reduced immunostaining intensity of all the proteins compared to the WT (Fig. 5I). At the 1-month stage, the difference between WT and Nell-1$^{Col2\alpha1}$KO mice was even more significant. The expression of Ihh (Fig. 5E), Patched-1 (Fig. 5F), PTHrP (Fig. 5G), and PTHrP-R (Fig. 5H) in the Nell-1$^{Col2\alpha1}$KO epiphyseal plate were all confined to a limited band of prehypertrophic and early hypertrophic chondrocytes, while the WT mice showed obviously wider distributions and more abundant expression (Fig. 5J). These reduced expressions *in vivo* were consistent with the protein expression levels observed in primary WT and Nell-1$^{Col2\alpha1}$KO chondrocytes, while application of exogenous rhNELL-1 significantly rescued these losses (Fig. 5K).

Therefore, the changes of distribution and staining intensity in the Nell-1$^{Col2\alpha1}$KO epiphyseal plate showed an Ihh-PTHrP signaling loop affected by Nell-1 inactivation, indicating the essential role of Nell-1 in endochondral ossification.

Exogenous Nell-1 restores affected proliferation and differentiation/maturation of chondrocytes in Nell-1$^{Col2\alpha1}$KO mice by elevating Ihh signaling

Having demonstrated alterations during endochondral ossification caused by Nell-1 inactivation *in vivo*, we then verified Nell-1's role on chondrocyte proliferation and differentiation *in vitro* to gain insight into a possible mechanism. In Nell-1$^{Col2\alpha1}$KO chondrocytes, the gene expression levels of Col-2 and Aggrecan were significantly reduced compared with WT after 14-day cultivation in chondrogenic medium (Fig. 6A). The same pattern of chondrogenic differentiation was also showed by Alcian blue staining (Fig. 6B). Not surprisingly, the key molecules of the Ihh signaling pathway were all down-regulated in primary chondrocytes isolated from Nell-1$^{Col2\alpha1}$KO mice at varying degrees (Fig. 6C). As expected, the application of exogenous rhNELL-1 significantly rescued the loss in gene expression of Col-2, Aggrecan, Ihh, Gli-1, as well as chondrogenic differentiation as revealed by Alcian blue staining in Nell-1$^{Col2\alpha1}$KO mice (Fig. 6A–C). In corroboration with our *in vivo* BrdU incorporation results, the MTT assay showed decreased proliferation of Nell-1$^{Col2\alpha1}$KO chondrocytes which could also be recovered by exogenous rhNELL-1 (Fig. 6D).

With the significant alterations of the Ihh-PTHrP signaling loop in the epiphyseal plate of Nell-1$^{Col2\alpha1}$KO mice, the importance of Nell-1 in Ihh-mediated chondrocyte differentiation seemed to be clear. To confirm this finding, we applied 2 different Ihh signaling inhibitors, cyclopamine for Smo and GANT61 for Gli-1, to study the interplay between Nell-1 and Ihh-PTHrP by observing the potential changes of chondrogenic differentiation and its relevant

molecules. After 3-day cultivation, the gene expression of Col-2, Aggrecan, and all studied key molecules in the Ihh-PTHrP signaling pathway were all significantly decreased in Nell-1$^{Col2\alpha1}$KO chondrocytes (Fig. 6E, F), in WT chondrocytes inhibited with cyclopamine (Fig. 6G, H), and in WT chondrocytes inhibited with GANT61 (Fig. 6I, J). Notably, the degree of recovery with rhNELL-1 application was quite different among the groups. For Nell-1$^{Col2\alpha1}$KO chondrocytes, rhNELL-1 application significantly increased the gene expression of all the studied markers except Smo (Fig. 6E, F). On the contrary, none of markers were rescued by rhNELL-1 when Smo was inhibited by cyclopamine in WT chondrocytes (Fig. 6G, H), while only Col-2, Ihh and Patched-1 were increased with application of rhNELL-1 in the WT+GANT61 group (Fig. 6I, J). Among all the tested molecules involved in the Ihh-PTHrP signaling pathway, Gli-1 was the most sensitive to Nell-1 in Nell-1$^{Col2\alpha1}$KO chondrocytes (Fig. 6C, F). Thus, we then observed Gli-1's nuclear expression on the protein level by ICC (Fig. 6K), and subsequently verified this by Western blot (Fig. 6L), since its nuclear accumulation is critical for function. Both of them showed greater nuclear Gli-1 expression in WT chondrocytes, while rhNELL-1 application clearly elevated the protein level of Gli-1 in the Nell-1$^{Col2\alpha1}$KO cell nucleus. Gli-1 expression was hardly detected in cytoplasmic fractions (Fig. 6L). Because of the importance of Gli-1 as a transcription factor in the Ihh signaling pathway, we further tested the expression of Gli-1's downstream target genes, Hip-1 and N-Myc. Expression of both increased with rhNELL-1 application in WT and Nell-1$^{Col2\alpha1}$KO chondrocytes, and decreased with Nell-1 inactivation in Nell-1$^{Col2\alpha1}$KO cells (Suppl Fig. S7A, B). When WT chondrocytes were treated with GANT61 to block Gli-1, rhNELL-1 application could no longer increase their expressions (Suppl Fig. S7B).

By aggregate, Nell-1 inactivation in Col-2 expressing chondrocytes rendered intrinsic deficits of Ihh signaling components, which in turn significantly affected chondrogenic differentiation and proliferation. Nell-1 recombinant protein can partially rescue the chondrogenic defects by affecting the Ihh signaling pathway, specifically by elevating nuclear Gli-1 protein.

Discussion

Among putative bone growth factors, Nell-1 is a relatively new member with great translational potential in skeletal regenerative medicine [6–10], and merits more extensive studies in supporting its development as a novel therapy for human skeletal conditions. In contrast to previous studies of Nell-1 on craniofacial bone development [1,13,15], we focused our efforts on investigating Nell-1's role in endochondral bone formation of the appendicular skeleton by successfully generating conditional Nell-1 knockout mice (Nell-1$^{Col2\alpha1}$KO). Significantly, the cumulative inactivation of Nell-1 in Col-2 expressing cells resulted in early onset of short stature, dwarfism, and premature osteoporosis with less cortical bone formation. These phenotypes were observed in neither neonatal nor postnatal heterozygous ENU-induced Nell-1 mutant mice [4,12,13]. The high similarity of the phenotypical findings from Nell-1$^{Col2\alpha1}$KO mice with the abnormalities reported for a human case affecting the Nell-1 gene locus implicated the functional importance of Nell-1 in the pathogenesis of human skeletal conditions beyond the craniofacial tissues [2,5]. Notably, no significant differences were observed between male and female mice in terms of the pathological

effects induced by Nell-1 deficiency. Col2α1-Cre transgenic mice, which served as a negative control, exhibited no significant differences with the WT control with regards skeletogenesis. By means of dynamic observation of morphological and molecular changes of the epiphyseal plate and secondary ossification center (SOC) at multiple postnatal stages, Nell-1 was definitively identified as an essential factor for maintaining normal homeostasis of the epiphyseal plate and the programmed progression of SOC for the first time. Further dissection of the molecular mechanisms by which Nell-1 plays critical roles in bone growth highly suggested that the Ihh-PTHrP signaling feedback loop was altered significantly, thereby affecting the proliferation and maturation of epiphyseal plate chondrocytes in Nell-1^{Col2α1}KO mice. Thus, this study has greatly advanced our understanding of Nell-1's functionalities and the underpinning mechanisms in regulating the growth of the appendicular bones and its associated abnormalities in mice, resulting in practical impacts to the translational aspects of Nell-1.

Nell-1 haploinsufficiency resulted in osteoporosis in 18-month-old ENU-induced Nell-1 deficient mice, but not in younger stage mice (P1, 1 month, and 6 months) [(4)]. In contrast, early onset of osteoporosis was clearly demonstrated in Nell-1^{Col2α1}KO mice at 1 month by high resolution micro-CT. Dynamic histomorphometric analysis of the metaphyseal trabecular bones further revealed discrepancies of the underlying mechanisms controlling both function and numbers of osteoblasts and osteoclasts between 1 and 3-month old mice due to cumulative inactivation of Nell-1 in Col-2 expressing cells, displaying Nell-1's role in maintaining a delicate balance of the osteogenic microenvironment. Less trabecular bone formation under the epiphyseal plate in Nell-1^{Col2α1}KO mice brought greater attention to the effects of Nell-1 on epiphyseal homeostasis. With the clear morphological observation of SOC development from day 7 to day 28, the lack of Nell-1 in chondrocytes may be one of the critical factors affecting initial formation of the SOC by inhibiting Runx2, VEGF, and Col-10 expression [(34–36)]. Runx2 has been well recognized as a major regulator of chondrocyte hypertrophy and Col-10 expression [(37)], while Nell-1 – as a direct downstream target of Runx2 in chondrocytes [(38)] – may also affect Runx2 activity through a feedback mechanism [(39)]. The inhibitory mechanism on Runx2 expression by Nell-1 inactivation in chondrocytes may involve a degree of crosstalk among active molecules in the SOC [(27,40–42)] rather than a straightforward transcriptional regulatory relationship between Runx2 and Nell-1 [(38,43)]. However, this study provided direct evidence of Nell-1's key role in the initiation and progression of SOC formation. In addition to the metaphyseal trabecular bones, decreased volume, thickness, and mineral density of femoral and tibial mid-shaft cortical bone in Nell-1^{Col2α1}KO mice may reveal new insight on cortical bone formation and remodeling when Nell-1 was inactivated, although the specific molecular mechanisms remained to be further explored.

Dwarfism with shortened limbs or chondrodysplasia was associated with several other factors by different mechanisms. It may occur with craniofacial abnormalities [(44,45)], which was also observed in Nell-1^{Col2α1}KO mice (unpublished data and out of the scope of this study). The inactivation of integrin-linked kinase (ILK) in chondrocytes resulted in obvious chondrodysplasia and dwarfism by reducing proliferation of epiphyseal plate chondrocytes but displayed normal chondrocyte differentiation [(46)]. In addition, hyperactivity of the mechanistic target of rapamycin (mTOR) complex1 (mTORC1) was responsible for

chondrodysplasia and dwarfism in mice by uncontrolled cell proliferation and blockage of differentiation within the epiphyseal plate [47]. Moreover, mice lacking link protein (LP) showed short-limb dwarfism and reduced mineralization at the secondary ossification center by altering the Ihh-PTHrP signaling pathway, as well as decreased chondrocyte differentiation but normal proliferation [44]. In contrast to ILK, mTORC1, and LP, the dwarfism with shortened limbs caused by inactivation of Nell-1 in chondrocytes came with reduced chondrocyte proliferation and affected chondrocyte differentiation. In particular, severely reduced Col-10 immunostaining in Nell-1$^{Col2\alpha1}$KO epiphyseal plates clearly indicated impairment of chondrocyte maturation. These phenotypes are consistent with previously reported Ihh deficient mutants which showed severe short-limb dwarfism, reduced chondrocyte proliferation, disorganized chondrocyte differentiation, and delayed and decreased cortical or trabecular bone formation in long bones with down-regulation of PTHrP and PTHrP-R expression [48–50]. Although the mechanism by which Ihh stimulates the production of PTHrP is poorly understood [24], the Ihh-PTHrP loop is required to maintain normal chondrocyte proliferation and differentiation together with bone formation during endochondral ossification [18–20,23,24,48,51].

Our current data show that chondrocyte-specific inactivation of Nell-1 had a prominent impact on the Ihh-PTHrP signaling loop. At the newborn stage, the synthesis of PTHrP in the perichondrial cells and chondrocytes at the end of the developing bones decreased with downregulated Ihh expression in the prehypertrophic and early hypertrophic chondrocytes caused by chondrocyte-specific Nell-1 inactivation. Reduced proliferation and differentiation of chondrocytes were observed in Nell-1$^{Col2\alpha1}$KO epiphyseal plates. Presumptively, there are two Ihh-PTHrP signaling loops in the postnatal epiphyseal plate, one confined to the prehypertrophic chondrocytes and one involving the epiphyseal plate stem cells [52]. In our study, 1-month WT epiphyseal cartilage exhibited wider distribution and stronger expression of Ihh, Ptch-1, PTHrP, and PTHrP-R, indicating greater interactions between Ihh and PTHrP and suggesting crosstalk between these two loops. However, Nell-1 deficiency resulted in limited Ihh-PTHrP loop in prehypertrophic/early hypertrophic zone with impaired proliferation and maturation of chondrocytes. Downregulated key molecules in the Ihh-PTHrP signaling pathway were also observed in Nell-1$^{Col2\alpha1}$KO primary chondrocytes *in vitro*. Furthermore, two distinct inhibitors of the Ihh signaling pathway were used to delineate the distinctive role of Nell-1 in modulating Ihh signaling. Cyclopamine can directly bind to the heptahelical bundle of Smo[53], while the binding of GANT61 to Gli-1 determines inhibition of Gli-DNA binding [54,55]. With different targets and effects caused by these two inhibitors, Nell-1 was confirmed to act through derepressed Smo as a major route for its involvement in Ihh signaling. (Fig. 7). However, it cannot be completely ruled out that an Ihh-independent mechanism [51,56–58] was also involved in mediating chondrocytes proliferation and differentiation in Nell-1$^{Col2\alpha1}$KO model.

Without a doubt, Nell-1 is not the only functional molecule that regulates bone growth and remodeling of the appendicular skeletons [16–19,23,24]. Thus, crosstalk and interplay among these functional factors warrants future investigation. Nonetheless, Nell-1 is indeed an essential factor in modulating epiphyseal homeostasis and appendicular skeletogenesis given its newly defined critical roles in affecting longitudinal bone growth, metaphyseal trabecular bone structure, and cortical bone volume and mineral density. In summary, the

Nell-1$^{Col2\alpha1}$KO mouse model exhibited dwarfism and premature osteoporotic phenotypes similar to a recent clinical report of short stature [5] and a Framingham study on human osteoporosis-related genes [3]. The key role of Nell-1 on the regulation of the Ihh-PTHrP signaling pathway was then demonstrated *in vivo* and *in vitro*. Moreover, these results were further supported by consistent phenotypes observed in Ihh deficient mutants [48–50]. With the proven chondrogenic applications of Nell-1 [7,29] and its established function as a secreted molecule upstream of Ihh [25], these findings offer additional opportunities for Nell-1's further in-depth mechanistic study and application.

Supplementary Material

Refer to Web version on PubMed Central for supplementary material.

Acknowledgements

We would like to thank Drs. Wenlu Jiang, Justine Tanjaya, Chenchao Wang, Xiaoxiao Pang, Chenshuang Li, and Zhong Zheng at the University of California, Los Angeles for their excellent technical assistance and scientific input.

Grant Support: This study was supported by the NIH/NIAMS (grants R01AR066782, R01AR068835, R01AR061399), NIH/NIDCR (grant K08DE026805), UCLA/NIH CTSI (grant UL1TR000124), the National Aeronautical and Space Administration ("NASA", GA-2014-154), and AAOF OFDFA award for J.H.K.

References

1. Zhang X, Kuroda SI, Carpenter D, Nishimura I, Soo C, Moats R, et al. Craniosynostosis in transgenic mice overexpressing Nell-1. Journal of Clinical Investigation. 2002;110(6):861–70. [PubMed: 12235118]
2. Ting K, Vastardis H, Mulliken JB, Soo C, Tieu A, Do H, et al. Human NELL-1 Expressed in Unilateral Coronal Synostosis. Journal of Bone and Mineral Research. 1999;14(1):80–9. [PubMed: 9893069]
3. Karasik D, Hsu YH, Zhou Y, Cupples LA, Kiel DP, Demissie S. Genome-wide pleiotropy of osteoporosis-related phenotypes: the Framingham Study. J Bone Miner Res. 7 2010;25(7):1555–63. [PubMed: 20200953]
4. James AW, Shen J, Zhang X, Asatrian G, Goyal R, Kwak JH, et al. NELL-1 in the treatment of osteoporotic bone loss. Nat Commun. 6 17 2015;6:7362. [PubMed: 26082355]
5. Dateki S, Watanabe S, Kinoshita F, Yoshiura KI, Moriuchi H. Identification of 11p14.1-p15.3 deletion probably associated with short stature, relative macrocephaly, and delayed closure of the fontanelles. Am J Med Genet A. 1 2017;173(1):217–20. [PubMed: 27662520]
6. Zhang X, Zara J, Siu RK, Ting K, Soo C. The Role of NELL-1, a Growth Factor Associated with Craniosynostosis, in Promoting Bone Regeneration. Journal of dental research. 7/20 2010;89(9): 865–78. [PubMed: 20647499]
7. Siu RK, Zara JN, Hou Y, James AW, Kwak J, Zhang X, et al. NELL-1 Promotes Cartilage Regeneration in an In Vivo Rabbit Model. Tissue Engineering Part A. 2012;18(3–4):252. [PubMed: 21902605]
8. Aghaloo T, Cowan CM, Chou YF, Zhang X, Lee H, Miao S, et al. Nell-1-induced bone regeneration in calvarial defects. American Journal of Pathology. 2006;169(3):903–15. [PubMed: 16936265]
9. Siu RK, Lu SS, Li W, Whang J, McNeill G, Zhang X, et al. Nell-1 protein promotes bone formation in a sheep spinal fusion model. Tissue Eng Part A. 4 2011;17(7–8):1123–35. [PubMed: 21128865]
10. Li W, Lee M, Whang J, Siu RK, Zhang X, Liu C, et al. Delivery of lyophilized Nell-1 in a rat spinal fusion model. Tissue Eng Part A. 9 2010;16(9):2861–70. [PubMed: 20528102]

11. James AW, Shen J, Tsuei R, Nguyen A, Khadarian K, Meyers CA, et al. NELL-1 induces Sca-1+ mesenchymal progenitor cell expansion in models of bone maintenance and repair. JCI Insight. 6 15 2017;2(12).
12. Desai J, Shannon ME, Johnson MD, Ruff DW, Hughes LA, Kerley MK, et al. Nell1-deficient mice have reduced expression of extracellular matrix proteins causing cranial and vertebral defects. Human Molecular Genetics. 2006;15(8):1329–41. [PubMed: 16537572]
13. Zhang X, Ting K, Pathmanathan D, Ko T, Chen W, Chen F, et al. Calvarial Cleidocraniodysplasia-like defects with ENU-induced Nell-1 deficiency. The Journal of Craniofacial Surgery. 2012;23(1): 61–6. [PubMed: 22337375]
14. Zhang X, Cowan CM, Jiang X, Soo C, Miao S, Carpenter D, et al. Nell-1 induces acrania-like cranioskeletal deformities during mouse embryonic development. Laboratory Investigation. Research Article 05/01/online 2006;86:633. [PubMed: 16652108]
15. Zhang X, Carpenter D, Bokui N, Soo C, Miao S, Truong T, et al. Overexpression of Nell-1, a Craniosynostosis-Associated Gene, Induces Apoptosis in Osteoblasts During Craniofacial Development. Journal of Bone and Mineral Research. 2003;18(12):2126–34. [PubMed: 14672347]
16. Mackie EJ, Tatarczuch L, Mirams M. The skeleton: a multi-functional complex organ: the growth plate chondrocyte and endochondral ossification. J Endocrinol. 11 2011;211(2):109–21. [PubMed: 21642379]
17. Hunziker EB. Mechanism of longitudinal bone growth and its regulation by growth plate chondrocytes. Microsc Res Tech. 8 15 1994;28(6):505–19. [PubMed: 7949396]
18. Olsen Bjorn R., Reginato Anthony M., Wang W. Bone Development. Annual Review of Cell and Developmental Biology. 2000;16(1):191–220.
19. Mackie EJ, Ahmed YA, Tatarczuch L, Chen KS, Mirams M. Endochondral ossification: how cartilage is converted into bone in the developing skeleton. Int J Biochem Cell Biol. 2008;40(1): 46–62. [PubMed: 17659995]
20. Yang J, Andre P, Ye L, Yang YZ. The Hedgehog signalling pathway in bone formation. Int J Oral Sci. 6 26 2015;7(2):73–9. [PubMed: 26023726]
21. Shi Y, Chen J, Karner CM, Long F. Hedgehog signaling activates a positive feedback mechanism involving insulin-like growth factors to induce osteoblast differentiation. Proc Natl Acad Sci U S A. 4 14 2015;112(15):4678–83. [PubMed: 25825734]
22. Alvarez J, Sohn P, Zeng X, Doetschman T, Robbins DJ, Serra R. TGFbeta2 mediates the effects of hedgehog on hypertrophic differentiation and PTHrP expression. Development. 4 2002;129(8): 1913–24. [PubMed: 11934857]
23. Ohba S Hedgehog Signaling in Endochondral Ossification. Journal of Developmental Biology. 2016;4(2):20.
24. Kronenberg HM. Developmental regulation of the growth plate. Nature. 10.1038/nature01657 05/15/print 2003;423(6937):332–6. [PubMed: 12748651]
25. Li C, Zheng Z, Zhang X, Asatrian G, Chen E, Song R, et al. Nfatc1 Is a Functional Transcriptional Factor Mediating Nell-1-Induced Runx3 Upregulation in Chondrocytes. Int J Mol Sci. 1 6 2018;19(1).
26. Li C, Zheng Z, Jiang J, Jiang W, Lee K, Berthiaume EA, et al. Neural EGFL-Like 1 Regulates Cartilage Maturation through Runt-Related Transcription Factor 3-Mediated Indian Hedgehog Signaling. Am J Pathol. 2 2018;188(2):392–403. [PubMed: 29137952]
27. Xing W, Cheng S, Wergedal J, Mohan S. Epiphyseal chondrocyte secondary ossification centers require thyroid hormone activation of Indian hedgehog and osterix signaling. Journal of bone and mineral research : the official journal of the American Society for Bone and Mineral Research. 2014;29(10):2262–75.
28. Kawamoto T, Kawamoto K. Preparation of Thin Frozen Sections from Nonfixed and Undecalcified Hard Tissues Using Kawamot's Film Method (2012) In: Hilton MJ, editor. Skeletal Development and Repair: Methods and Protocols. Totowa, NJ: Humana Press; 2014 p. 149–64.
29. Lee M, Siu RK, Ting K, Wu BM. Effect of Nell-1 delivery on chondrocyte proliferation and cartilaginous extracellular matrix deposition. Tissue Engineering Part A. 2010;16(5):1791–800. [PubMed: 20028218]

30. Dao DY, Jonason JH, Zhang Y, Hsu W, Chen D, Hilton MJ, et al. Cartilage-specific β-CATENIN signaling regulates chondrocyte maturation, generation of ossification centers, and perichondrial bone formation during skeletal development. Journal of Bone and Mineral Research. 2012;27(8): 1680–94. [PubMed: 22508079]

31. Gao L, Sheu TJ, Dong Y, Hoak DM, Zuscik MJ, Schwarz EM, et al. TAK1 regulates SOX9 expression in chondrocytes and is essential for postnatal development of the growth plate and articular cartilages. J Cell Sci. 12 15 2013;126(Pt 24):5704–13. [PubMed: 24144697]

32. Shen J, James AW, Zhang X, Pang S, Zara JN, Asatrian G, et al. Novel Wnt Regulator NEL-Like Molecule-1 Antagonizes Adipogenesis and Augments Osteogenesis Induced by Bone Morphogenetic Protein 2. Am J Pathol. 2 2016;186(2):419–34. [PubMed: 26772960]

33. Ovchinnikov DA, Deng JM, Ogunrinu G, Behringer RR. Col2a1-directed expression of Cre recombinase in differentiating chondrocytes in transgenic mice. genesis. 2000;26(2):145–6. [PubMed: 10686612]

34. Laurie LE, Kokubo H, Nakamura M, Saga Y, Funato N. The Transcription Factor Hand1 Is Involved In Runx2-Ihh-Regulated Endochondral Ossification. PLoS One. 2016;11(2):e0150263. [PubMed: 26918743]

35. Jones DC, Schweitzer MN, Wein M, Sigrist K, Takagi T, Ishii S, et al. Uncoupling of growth plate maturation and bone formation in mice lacking both Schnurri-2 and Schnurri-3. Proc Natl Acad Sci U S A. 5 4 2010;107(18):8254–8. [PubMed: 20404140]

36. Chen M, Zhu M, Awad H, Li TF, Sheu TJ, Boyce BF, et al. Inhibition of beta-catenin signaling causes defects in postnatal cartilage development. J Cell Sci. 5 1 2008;121(Pt 9):1455–65. [PubMed: 18397998]

37. Ding M, Lu Y, Abbassi S, Li F, Li X, Song Y, et al. Targeting Runx2 expression in hypertrophic chondrocytes impairs endochondral ossification during early skeletal development. J Cell Physiol. 10 2012;227(10):3446–56. [PubMed: 22223437]

38. Li C, Jiang J, Zheng Z, Lee KS, Zhou Y, Chen E, et al. Neural EGFL-Like 1 Is a Downstream Regulator of Runt-Related Transcription Factor 2 in Chondrogenic Differentiation and Maturation. Am J Pathol. 5 2017;187(5):963–72. [PubMed: 28302495]

39. Zhang X, Ting K, Bessette CM, Culiat CT, Sung SJ, Lee H, et al. Nell-1, a key functional mediator of Runx2, partially rescues calvarial defects in Runx2(+/−) mice. J Bone Miner Res. 4 2011;26(4): 777–91. [PubMed: 20939017]

40. Zuscik MJ, Hilton MJ, Zhang X, Chen D, O'Keefe RJ. Regulation of chondrogenesis and chondrocyte differentiation by stress. J Clin Invest. 2 2008;118(2):429–38. [PubMed: 18246193]

41. van der Eerden BC, Karperien M, Wit JM. Systemic and local regulation of the growth plate. Endocr Rev. 12 2003;24(6):782–801. [PubMed: 14671005]

42. Lefebvre V, Smits P. Transcriptional control of chondrocyte fate and differentiation. Birth Defects Res C Embryo Today. 9 2005;75(3):200–12. [PubMed: 16187326]

43. Truong T, Zhang X, Pathmanathan D, Soo C, Ting K. Craniosynostosis-Associated Gene Nell-1 Is Regulated by Runx2. Journal of Bone and Mineral Research. 2007;22(1):7–18. [PubMed: 17042739]

44. Watanabe H, Yamada Y. Mice lacking link protein develop dwarfism and craniofacial abnormalities. Nat Genet. 2 1999;21(2):225–9. [PubMed: 9988279]

45. Holmbeck K, Bianco P, Caterina J, Yamada S, Kromer M, Kuznetsov SA, et al. MT1-MMP-Deficient Mice Develop Dwarfism, Osteopenia, Arthritis, and Connective Tissue Disease due to Inadequate Collagen Turnover. Cell. 99(1):81–92. [PubMed: 10520996]

46. Terpstra L, Prud'homme J, Arabian A, Takeda S, Karsenty G, Dedhar S, et al. Reduced chondrocyte proliferation and chondrodysplasia in mice lacking the integrin-linked kinase in chondrocytes. J Cell Biol. 7 7 2003;162(1):139–48. [PubMed: 12835312]

47. Yan B, Zhang Z, Jin D, Cai C, Jia C, Liu W, et al. mTORC1 regulates PTHrP to coordinate chondrocyte growth, proliferation and differentiation. Nat Commun. 4 4 2016;7:11151. [PubMed: 27039827]

48. St-Jacques B, Hammerschmidt M, McMahon AP. Indian hedgehog signaling regulates proliferation and differentiation of chondrocytes and is essential for bone formation. Genes & Development. 05/21/received 07/07/accepted 1999;13(16):2072–86. [PubMed: 10465785]

49. Maeda Y, Nakamura E, Nguyen MT, Suva LJ, Swain FL, Razzaque MS, et al. Indian Hedgehog produced by postnatal chondrocytes is essential for maintaining a growth plate and trabecular bone. Proc Natl Acad Sci U S A. 4 10 2007;104(15):6382–7. [PubMed: 17409191]
50. Razzaque MS, Soegiarto DW, Chang D, Long F, Lanske B. Conditional deletion of Indian hedgehog from collagen type 2alpha1-expressing cells results in abnormal endochondral bone formation. J Pathol. 12 2005;207(4):453–61. [PubMed: 16278811]
51. Karp SJ, Schipani E, St-Jacques B, Hunzelman J, Kronenberg H, McMahon AP. Indian hedgehog coordinates endochondral bone growth and morphogenesis via parathyroid hormone related-protein-dependent and -independent pathways. Development. 2 2000;127(3):543–8. [PubMed: 10631175]
52. van der Eerden BC, Karperien M, Gevers EF, Lowik CW, Wit JM. Expression of Indian hedgehog, parathyroid hormone-related protein, and their receptors in the postnatal growth plate of the rat: evidence for a locally acting growth restraining feedback loop after birth. J Bone Miner Res. 6 2000;15(6):1045–55. [PubMed: 10841173]
53. Chen JK, Taipale J, Cooper MK, Beachy PA. Inhibition of Hedgehog signaling by direct binding of cyclopamine to Smoothened. Genes Dev. 11 1 2002;16(21):2743–8. [PubMed: 12414725]
54. Lauth M, Bergstrom A, Shimokawa T, Toftgard R. Inhibition of GLI-mediated transcription and tumor cell growth by small-molecule antagonists. Proc Natl Acad Sci U S A. 5 15 2007;104(20): 8455–60. [PubMed: 17494766]
55. Agyeman A, Jha BK, Mazumdar T, Houghton JA. Mode and specificity of binding of the small molecule GANT61 to GLI determines inhibition of GLI-DNA binding. Oncotarget. 6 30 2014;5(12):4492–503. [PubMed: 24962990]
56. Minina E, Wenzel HM, Kreschel C, Karp S, Gaffield W, McMahon AP, et al. BMP and Ihh/PTHrP signaling interact to coordinate chondrocyte proliferation and differentiation. Development. 11 2001;128(22):4523–34. [PubMed: 11714677]
57. Minina E, Kreschel C, Naski MC, Ornitz DM, Vortkamp A. Interaction of FGF, Ihh/Pthlh, and BMP signaling integrates chondrocyte proliferation and hypertrophic differentiation. Dev Cell. 9 2002;3(3):439–49. [PubMed: 12361605]
58. Mak KK, Kronenberg HM, Chuang PT, Mackem S, Yang Y. Indian hedgehog signals independently of PTHrP to promote chondrocyte hypertrophy. Development. 6 2008;135(11): 1947–56. [PubMed: 18434416]

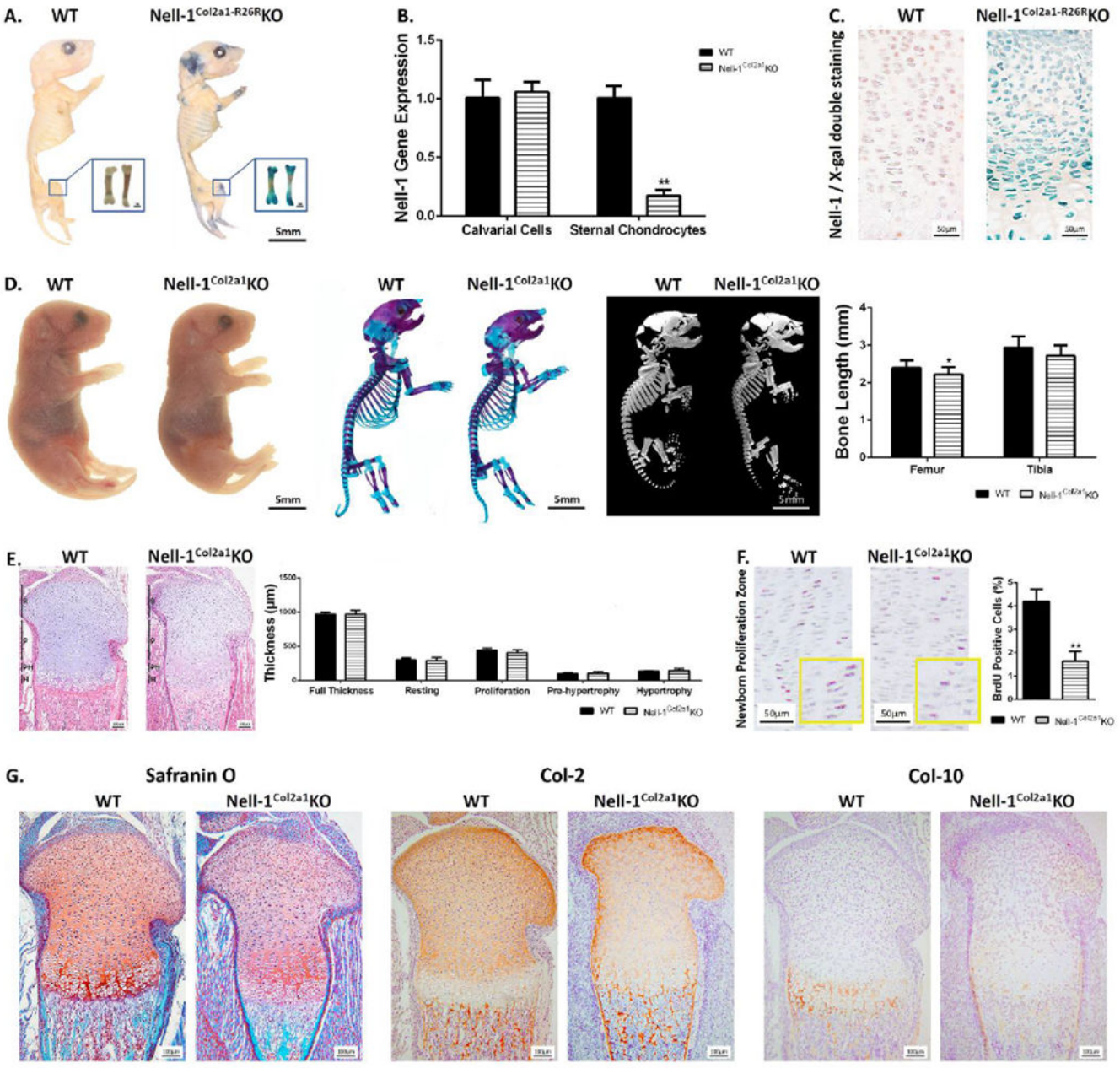

Figure 1. Generation of mutant mice with Nell-1-specific inactivation in Col2α1 expressing chondrocytes

(**A**) Positive X-gal staining in cartilage showed by whole-mount staining in neonatal Nell-1$^{Col2a1\text{-}R26R}$KO mice; (**B**) Decreased Nell-1 gene expression in primary Nell-1^{Col2a1}KO chondrocytes but not in primary calvarial cells, N=3; (**C**) Nell-1 deletion at the tissue level demonstrated by double staining of Nell-1 and X-gal on epiphyseal plates; (**D**) Gross appearance of Nell-1^{Col2a1}KO mutants at the newborn stage along with Alcian Blue-Alizarin Red skeletal staining, and 3D skeletal reconstructions, demonstrating subtle shortness of the limbs of newborn Nell-1^{Col2a1}KO mice, N=5; (**E**) H&E staining for newborn epiphyseal plates and no difference in zonal chondrocyte band widths with Nell-1

inactivation, N=5; **(F)** Significantly fewer BrdU positive cells were observed in the proliferative zone of newborn Nell-1^{Col2a1}KO mice, N=5; **(G)** Drastically reduced staining intensities of Safranin O, Col-2, and Col-10 in newborn Nell-1^{Col2a1}KO samples; R=Resting Zone, P=Proliferation Zone, PH=Pre-hypertrophy Zone, H=Hypertrophy Zone; *P<0.05; **P<0.01.

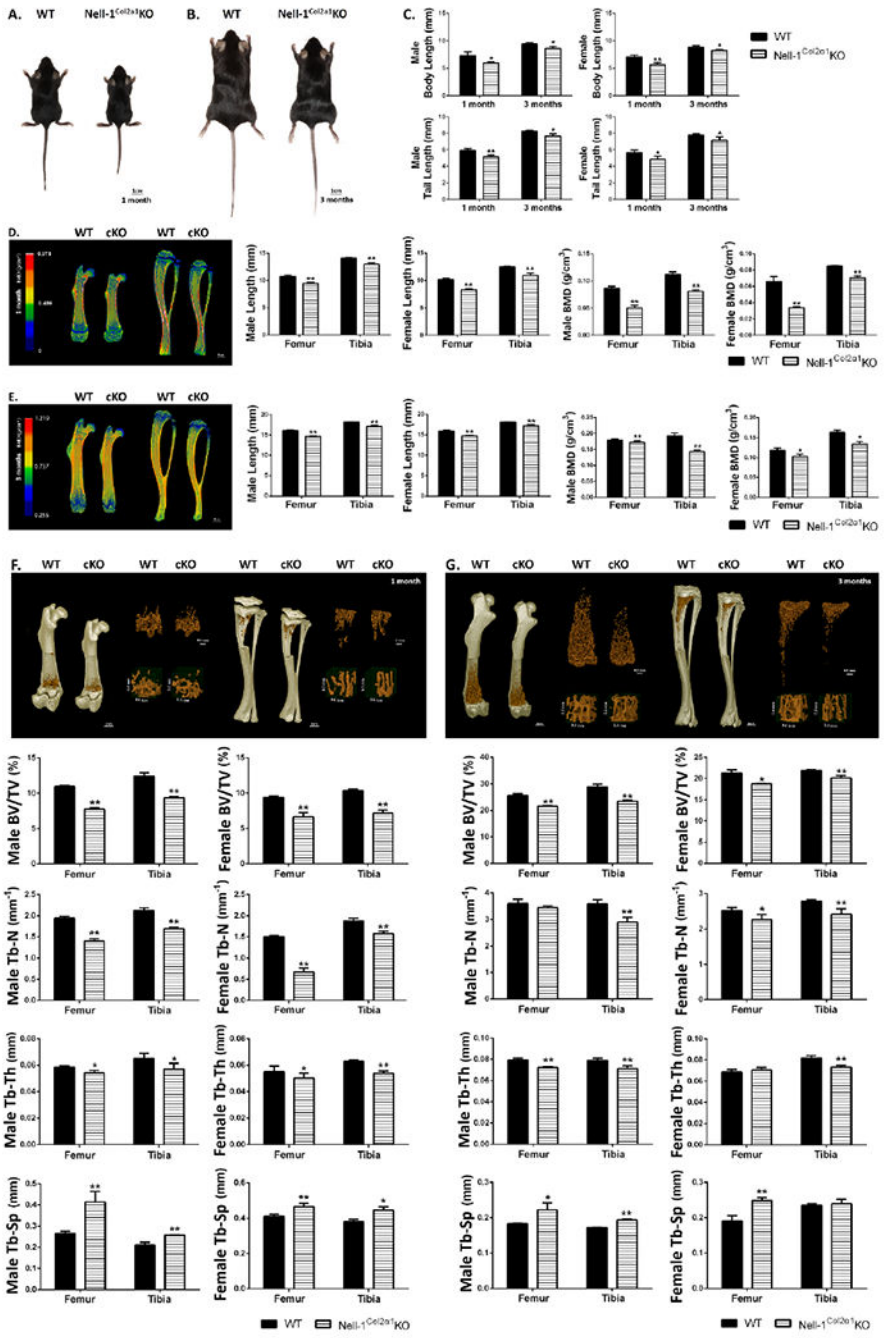

Figure 2. Dwarfism and premature osteoporotic phenotypes in Nell-1^{Col2a1}KO mice.

Gross appearance of a pair of (**A**) 1-month and (**B**) 3-month WT and Nell-1^{Col2a1}KO mice; (**C**) Significantly shorter body lengths and tail lengths were observed in male and female Nell-1^{Col2a1}KO mice; The femur and tibia length and bone mineral density in both male and female (**D**) 1-month and (**E**) 3-month Nell-1^{Col2a1}KO mice were much shorter as quantified by micro-CT; The distal femur and proximal tibia exhibited osteoporotic phenotypes in Nell-1^{Col2a1}KO mice at (**F**) 1 month and (**G**) 3 months with significantly reduced BV/TV,

Tb-N and Tb-Th, but increased Tb-Sp; The representative micro-CT images shown in this figure are from male mice; cKO=Nell-1$^{Col2\alpha1}$KO; N=5; *P<0.05; **P<0.01.

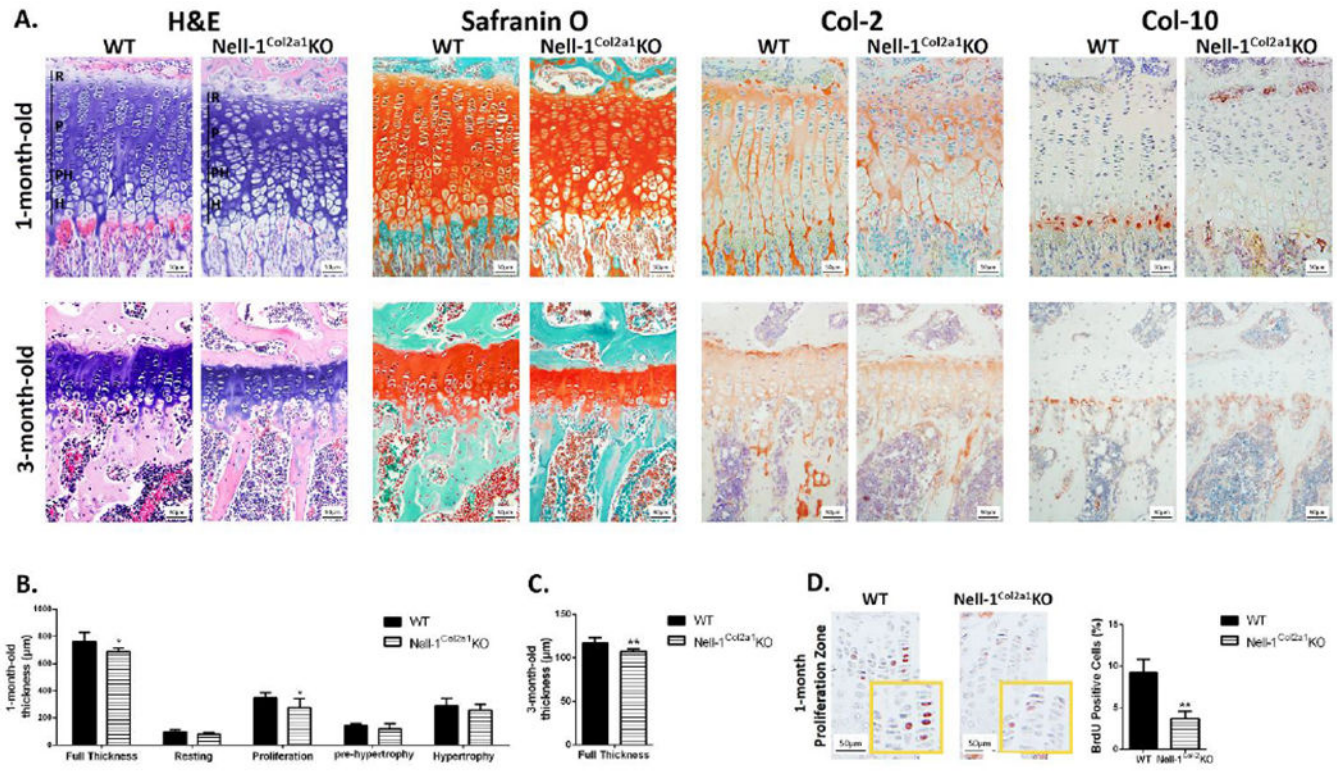

Figure 3. Histological changes observed in Nell-1^{Col2a1}KO mice epiphyseal plates.

(**A**) Altered thickness of epiphyseal plates and chondrocyte organization in 1-month and 3-month Nell-1^{Col2a1}KO mice as evidenced by H&E staining, in addition to reduced expression of the chondrogenic markers, Safranin O, Col-2 and Col-10; (**B**) The thickness of the proliferative zone and the full epiphyseal plates were significantly decreased in 1-month Nell-1^{Col2a1}KO mice; (**C**) The thickness of the full epiphyseal plates were reduced in 3-month Nell-1^{Col2a1}KO mice; (**D**) Significantly fewer BrdU positive cells were observed in the proliferative zone of epiphyseal plate in 1-month Nell-1^{Col2a1}KO mice; For the parameters shown in this figure, only male mice were used; R=Resting Zone, P=Proliferation Zone, PH=Pre-hypertrophy Zone, H=Hypertrophy Zone; N=5; *P<0.05; **P<0.01.

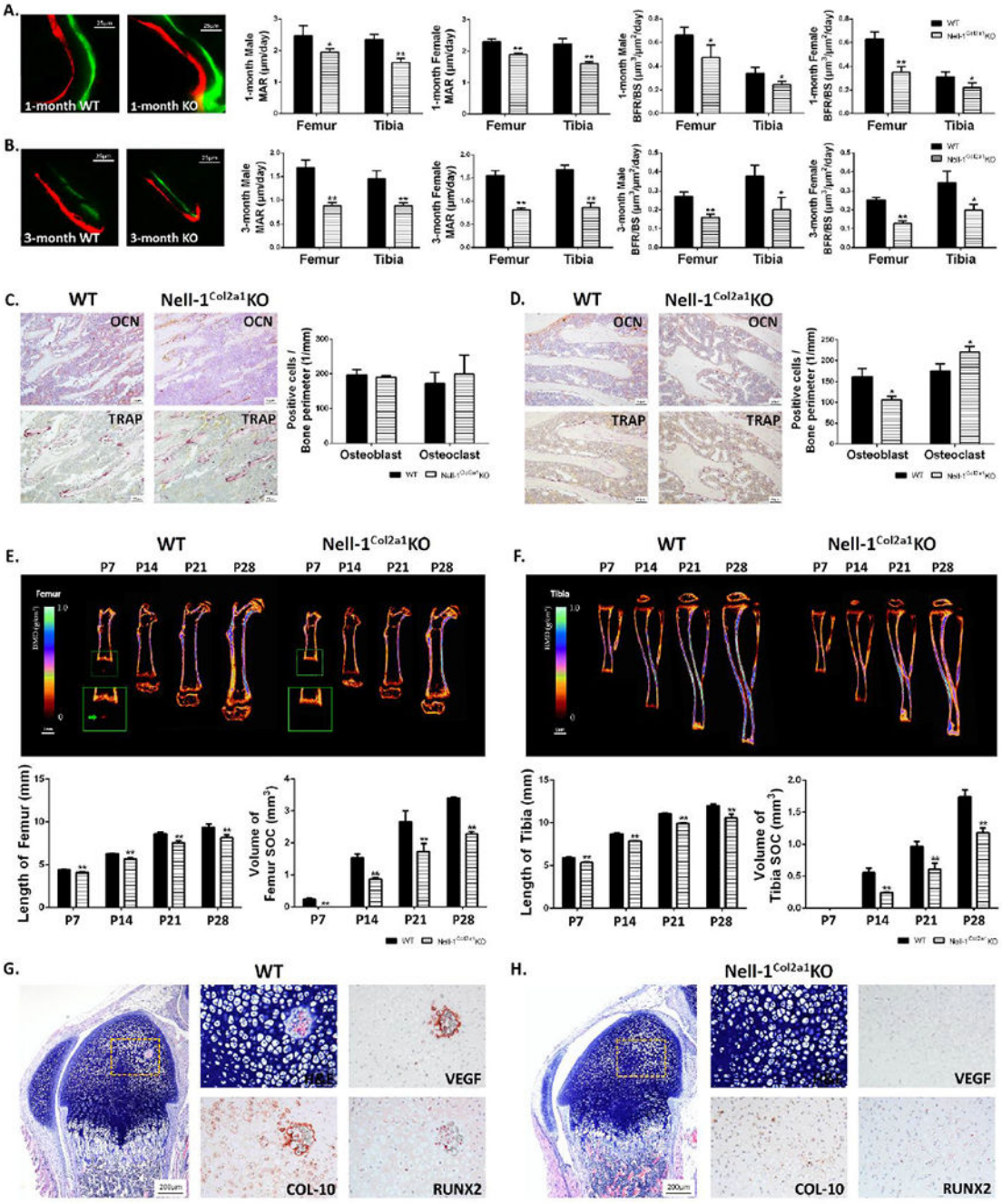

Figure 4. Reduced bone growth rate and delayed formation of secondary ossification centers in Nell-1^{Col2a1}KO mutants.

Significantly decreased MAR and BFR/BS in **(A)** 1-month and **(B)** 3-month Nell-1^{Col2a1}KO mice were measured by bone labelling, with similar patterns observed in male and female mice; Quantifications based on OCN and TRAP staining showed no significant difference in **(C)** 1-month Nell-1^{Col2a1}KO mice, but showed significantly reduced OB and increased OC at **(D)** 3 months; Delayed and smaller SOC formation and decreased limb lengths based on longitudinal measurements by in vivo micro-CT at different postnatal time points were

observed in the **(E)** femur and **(F)** tibia of Nell-1^{Col2a1}KO mice; Significantly altered intensity and distribution of VEGF, Col-10, and Runx2 immunostaining were observed at postnatal day 7 of the initial stage of SOC formation in **(G)** WT and **(H)** Nell-1^{Col2a1}KO mice; For the parameters shown in C-H, only male mice were used; N=5; *P<0.05; **P<0.01.

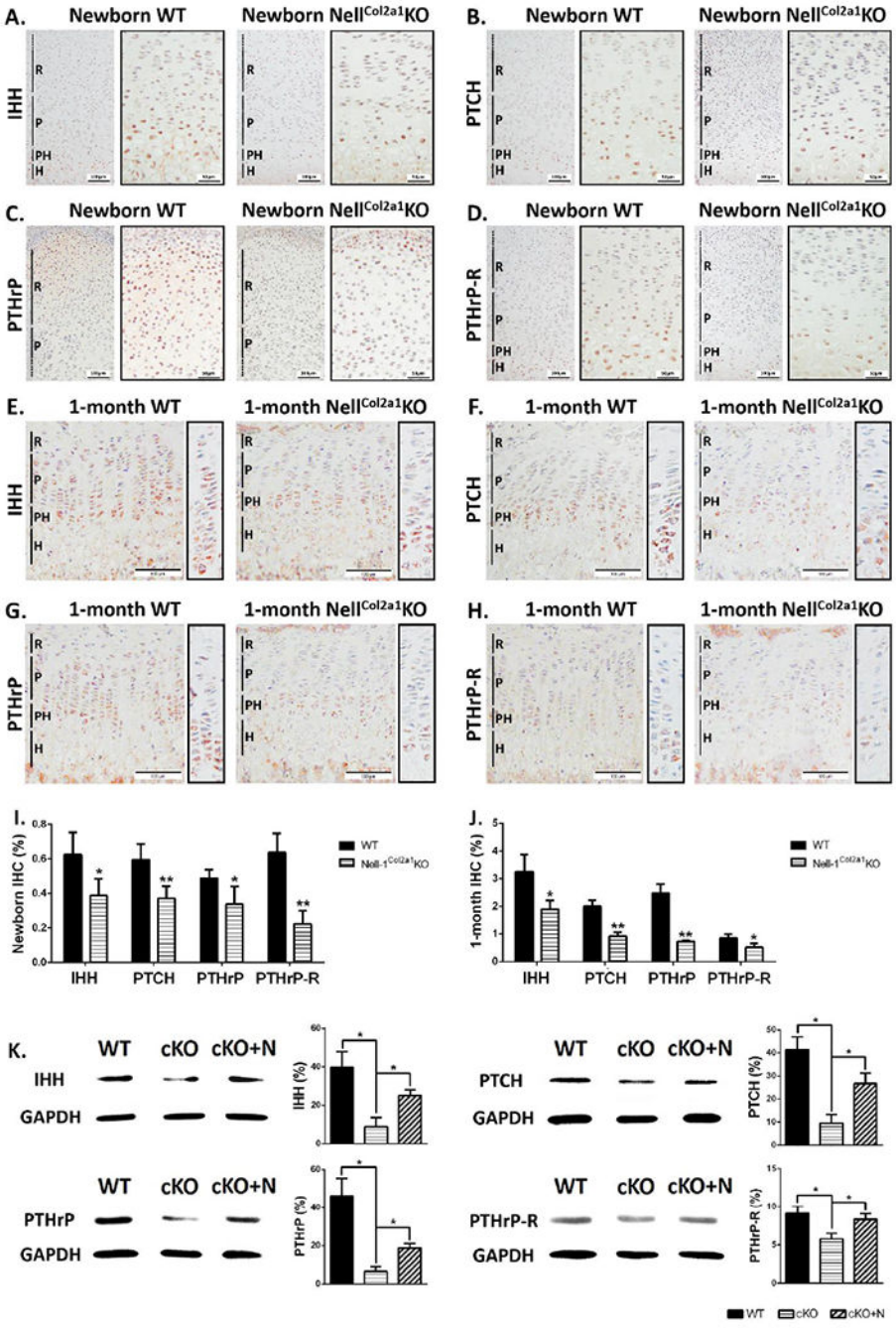

Figure 5. Decreased expression of key molecules involved in the Ihh-PTHrP loop in postnatal Nell-1^{Col2a1}KO epiphyseal plates.

As shown by IHC, in newborn Nell-1^{Col2a1}KO epiphyseal plates, decreased expressions of **(A)** Ihh, **(B)** Patched-1, and **(D)** PTHrP-R were all observed in the prehypertrophic and early hypertrophic chondrocytes, while less **(C)** PTHrP was expressed in perichondrial cells and resting chondrocytes; At the 1-month stage, the expressions of **(E)** Ihh, **(D)** Patched-1, **(F)** PTHrP, and **(H)** PTHrP-R in the Nell-1^{Col2α1}KO epiphyseal plates were all confined to a limited band of prehypertrophic and early hypertrophic chondrocytes, while the WT mice

showed obviously wider distributions and stronger expressions; Semi-quantification for these markers of IHC in **(I)** newborn and **(J)** 1-month mice showed significant decreases in expression, N=5; **(K)** Western Blot analyses showed decreased protein expression levels of Ihh, Patched-1, PTHrP, and PTHrP-R in primary WT and Nell-1$^{Col2\alpha1}$KO chondrocytes, while application of exogenous rhNELL-1 significantly rescued this loss, N=3; R=Resting Zone, P=Proliferation Zone, PH=Pre-hypertrophy Zone, H=Hypertrophy Zone, PTCH=Patched-1, cKO=Nell-1$^{Col2\alpha1}$KO, cKO+N=Nell-1$^{Col2\alpha1}$KO+rhNELL-1; *P<0.05; **P<0.01

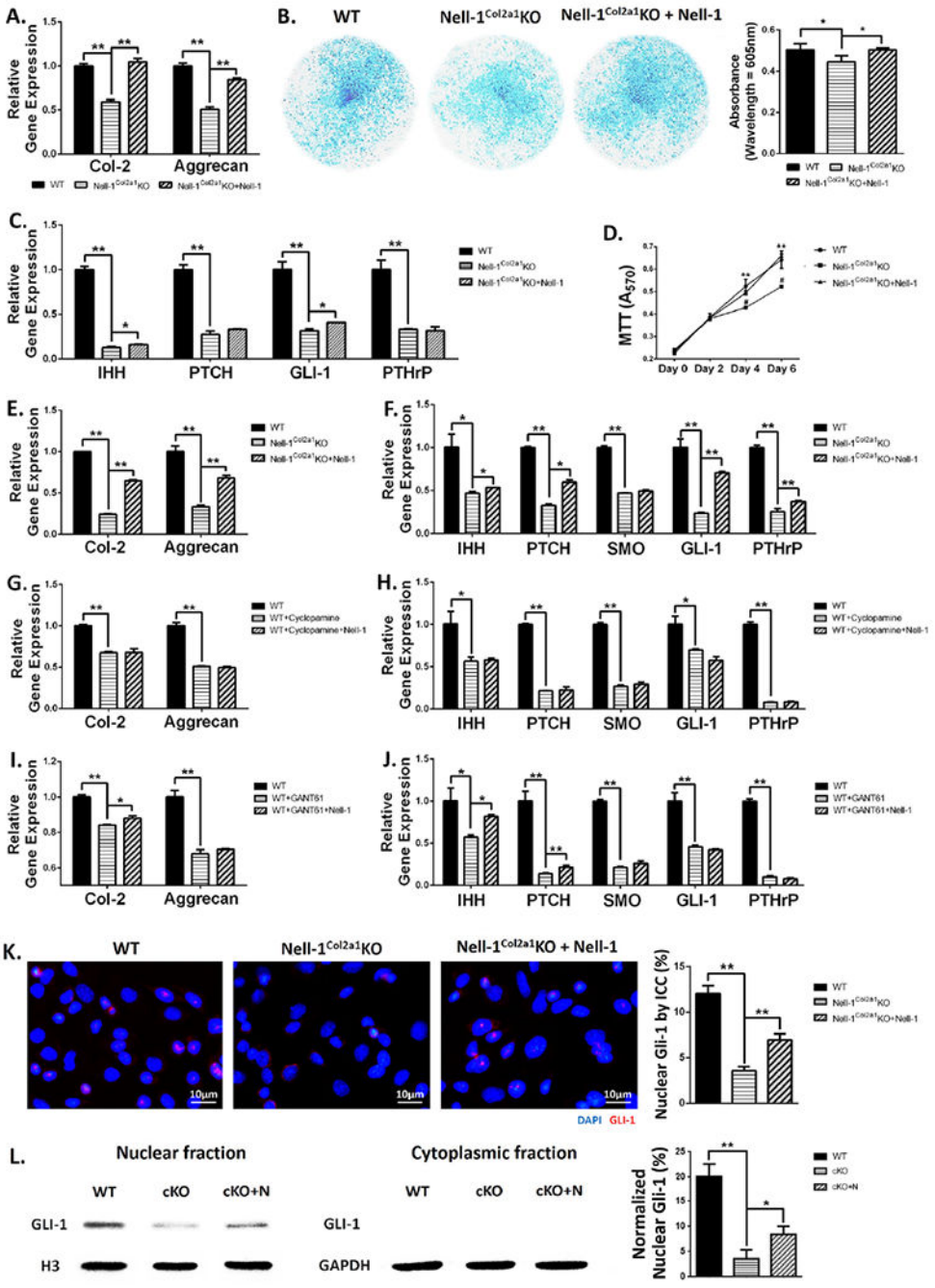

Figure 6. Nell-1 promotes chondrocyte proliferation and differentiation through predominantly modulating Ihh-PTHrP signaling.

Primary Nell-1^{Col2a1}KO chondrocytes showed **(A)** decreased gene expression of Col-2 and Aggrecan, **(B)** weaker Alcian blue staining intensity, **(C)** reduced gene expression of key molecules in the Ihh-PTHrP signaling pathway after 14-day chondrogenic cultivation, and **(D)** lower proliferation shown by the MTT assay, which were partially rescued by application of rhNELL-1; **(E, F)** Reduced gene expressions in Nell-1^{Col2a1}KO chondrocytes cultured in growth medium for 3 days increased with application of rhNELL-1; **(G, H)** The

rescued effects of rhNELL-1 were diminished when WT chondrocytes were treated with cyclopamine to block Smo; **(I, J)** When Gli-1 was blocked by GANT61, rhNELL-1 application only increased the expression of Ihh, Patched-1 and Col-2; **(K)** Decreased nuclear Gli-1 expression in Nell-1^{Col2a1}KO chondrocytes was revealed by immunocytochemistry, but can be compensated with application of rhNELL-1; **(L)** Gli-1 protein was hardly detected in the cytoplasmic fraction. Application of rhNELL-1 elevated the protein level of Gli-1 in the Nell-1^{Col2α1}KO cell nucleus as demonstrated by Western Blot; PTCH=Patched-1, SMO=Smoothened, cKO=Nell-1^{Col2α1}KO, cKO +N=Nell-1^{Col2α1}KO+rhNELL-1; N=3; *P<0.05; **P<0.01.

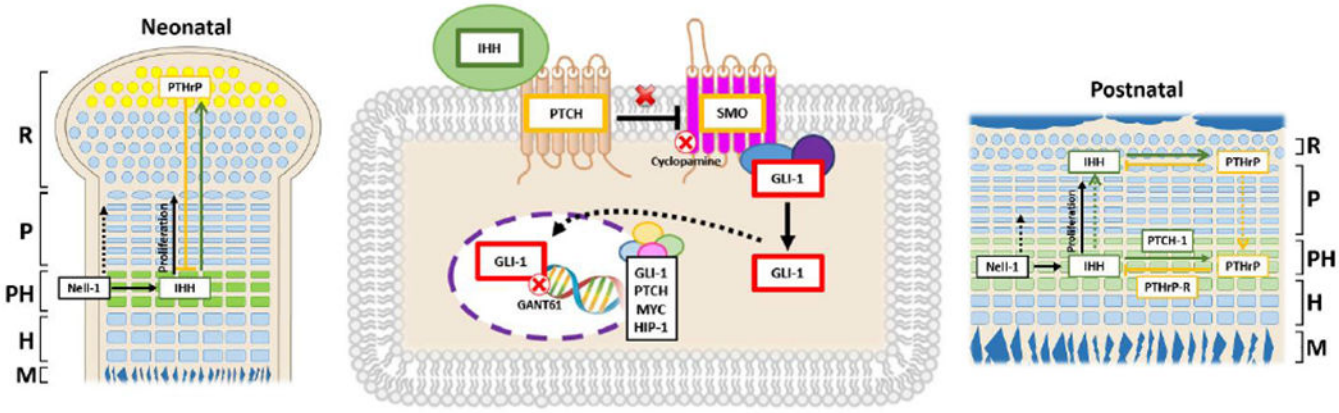

Figure 7. Schematic diagram of the interplay between Nell-1 and the Ihh-PTHrP signaling loop.

Binding of Ihh to its receptor, Patched-1, results in derepression of Smoothened, which can mediate dissociation of Gli-1. Nuclear accumulation of Gli-1 is critical for its function as a transcription factor to induce expression of target genes such as Gli-1, Patched-1, N-Myc, and Hip-1. Different effects by blocking Smoothened with cyclopamine and by blocking Gli-1 with GANT61 indicates that Nell-1 mainly acts through derepressed Smoothened **(middle panel)**. Notably, our data indicated that Nell-1 is critical in mediating the expression of PTHrP of chondrocytes at the ends of long bones at the neonatal stage, directly or by modulating Ihh, through a poorly understood mechanism **(left panel)**. At the postnatal stage, Nell-1 inactivation severely affects the number of positive cells and the protein expression levels of Ihh, PTHrP, and their receptors in the pre-hypertrophic zone as well as the proliferative activity of the proliferation zone likely through modulating Ihh-PTHrP signaling loop **(right panel)**; R=Resting Zone, P=Proliferation Zone, PH=Pre-hypertrophy Zone, H=Hypertrophy Zone, M=Mineralization Zone, PTCH=Patched-1, SMO=Smoothened.